Mon. Not. R. Astron. Soc. **000**, 1–10 (2002) Printed 1 February 2008 (MN LATEX style file v2.2)

The first rotation periods in Praesepe

Alexander Scholz[1⋆] and Jochen Eislöffel[2]†
[1] *SUPA, School of Physics & Astronomy, University of St. Andrews, North Haugh, St. Andrews, Fife KY16 9SS, United Kingdom*
[2] *Thüringer Landessternwarte Tautenburg, Sternwarte 5, D-07778 Tautenburg, Germany*

Accepted. Received.

ABSTRACT
The cluster Praesepe (age ~ 650 Myr) is an ideal laboratory to study stellar evolution. Specifically, it allows us to trace the long-term decline of rotation and activity on the main-sequence. Here we present rotation periods measured for five stars in Praesepe with masses of $0.1 - 0.5\,M_{\odot}$ – the first rotation periods for members of this cluster. Photometric periodicities were found from two extensive monitoring campaigns, and are confirmed by multiple independent test procedures. We attribute these variations to magnetic spots co-rotating with the objects, thus indicating the rotation period. The five periods, ranging from 5 to 84 h, show a clear positive correlation with object mass, a trend which has been reported previously in younger clusters. When comparing with data for F-K stars in the coeval Hyades, we find a dramatic drop in the periods at spectral type K8-M2 (corresponding to $0.4 - 0.6\,M_{\odot}$). A comparison with periods of VLM stars in younger clusters provides a constraint on the spin-down timescale: We find that the exponential rotational braking timescale is clearly longer than 200 Myr, most likely 400-800 Myr. These results are not affected by the small sample size in the rotation periods in Praesepe. Both findings, the steep drop in the period-mass relation and the long spin-down timescale, indicate a substantial change in the angular momentum loss mechanism for very low mass (VLM) objects, possibly the breakdown of the solar-type (Skumanich) rotational braking. While the physical origin for this behaviour is unclear, we argue that parts of it might be explained by the disappearance of the radiative core and the resulting breakdown of an interface-type dynamo in the VLM regime. Rotational studies in this mass range hold great potential to probe magnetic properties and interior structure of main-sequence stars.

Key words: stars: low-mass, brown dwarfs, stars: rotation, stars: evolution, stars: activity

1 INTRODUCTION

Clusters are ideal environments to study the evolution of stars. Members of one particular cluster share age, distance, as well as metallicity, and these parameters are typically well-constrained. Thus, clusters provide 'snapshots' of the stellar population at a given age. Comparing the properties of stars in clusters of different ages allows us then to track their evolution. Furthermore, clusters are often dense enough to allow multiplexed observations, i.e. wide-field imaging or multi-object spectroscopy, covering a large sample of objects simultaneously.

Two key parameters of stars, which strongly depend on age, are rotation and magnetic activity. The fundament for the understanding of the main-sequence evolution of rotation and activity is the empirically found Skumanich law: Looking at averages of large samples of objects, the rotational velocities of F to K stars evolve proportional to the inverse squareroot of age (e.g., Skumanich 1972; Barnes 2001). An analogous decline is seen for indicators of magnetic activity, implying a correlation between rotation and activity, which has been confirmed in multiple studies (e.g., Stauffer et al. 1997; Terndrup et al. 2000). This is usually interpreted with a twofold connection between stellar rotation and magnetic activity, providing a strong coupling between those two parameters: a) The interior dynamo of F-K stars, i.e. the underlying mechanism to generate magnetic activity, is thought to be governed by rotation. b) The rotational braking on the main-sequence is due to angular momentum losses through magnetic stellar winds (see Schrijver & Zwaan 2000).

To explain the presence of large-scale, stable magnetic fields in solar-type stars, it is usually assumed that the dynamo in F-K stars is similar to the solar-type $\alpha\omega$ dynamo and operates in the transition layer between the convective

⋆ E-mail: as110@st-andrews.ac.uk
† E-mail: jochen@tls-tautenburg.de

envelope and the radiative core. Therefore, it is expected that the magnetic field generation, and thus the magnetic and rotational properties, change when objects become fully convective at masses $< 0.3 - 0.4\,M_{\odot}$ (Chabrier & Baraffe 1997). However, no clear change of rotation and activity indicators has yet been detected at or around this mass limit (e.g., Delfosse et al. 1998). In addition, it is unclear what type of magnetic field is harboured by fully convective objects, and if it depends on rotation. Investigating the rotational evolution and angular momentum loss of very low mass (VLM) objects on the main-sequence can contribute to clarify these issues.

An ideal laboratory to analyse the rotation of VLM main-sequence stars is Praesepe: With an age probably between 0.6 and 0.9 Gyr (see Mermilliod 1981; Adams et al. 2002), the cluster is significantly older than zero age main sequence (ZAMS) clusters like the Pleiades or α Per. At these ages, all stars have safely arrived on the main-sequence and the rotational regulation is thus dominated by magnetic wind braking, and not anymore affected by initial conditions, disk-braking, and contraction – the objects have essentially 'forgotten' their pre-main sequence history. Thus, it is possible to isolate the effect of wind braking on the rotational properties.

Compared with the similarly old clusters Hyades and Coma, Praesepe is relatively compact, yet not too far away (180 pc, Robichon et al. 1999), allowing us deep, efficient observations with wide-field facilities. Here we report on photometric monitoring for 18 members of Praesepe, which provided the first five rotation periods for members of this cluster – all for objects with estimated masses below $0.5\,M_{\odot}$. Combined with previously published periods for younger objects (Scholz & Eislöffel 2004a,b, 2005), this allow us to probe the long-term evolution of rotation in the VLM regime.[1]

2 PHOTOMETRIC MONITORING

2.1 Observations

The analysis in this paper is based on two photometric time series of VLM stars in Praesepe. The observing strategy in both runs was similar: To mimimize internal inconsistencies in the data and thus systematic uncertainties, we 'stared' at a particular field in Praesepe. We did not 'dither' around a central position and made an effort to position the field of view at the same coordinates in each observing night. Therefore each object was at roughly the same pixel position on the detector throughout the run. The exposure time for the single frames was 600 sec in both runs. Since we were interested in very low mass objects, which have a spectral energy distribution peaking in the near-infrared, all observations were carried out in the I-band filter.

The target fields were selected to maximise the number of known Praesepe members in the field of view. We compiled an initial catalogue of VLM members from the surveys of Hambly et al. (1995a,b); Pinfield et al. (1997); Magazzu et al. (1998), at the time of the observations (2001, 2003) essentially the complete census of the VLM population in this cluster. For all these objects, the main criterium for cluster membership is multi-colour photometry, confirmed in many cases by proper motions and/or spectroscopy. According to a follow-up study by Hodgkin et al. (1999), the contamination rate is $\sim 10\%$ in the Hambly et al. sample and $\sim 50\%$ among the (fainter) Pinfield et al. objects.

Table 1. Logfile of the time series observations: Run, date of observations, no. of images, typical seeing

Run	Date	No.	Seeing
TLS	16/01/2001	12	$2\farcs0$
	17/01/2001	12	$2\farcs5$
	18/01/2001	6	$2\farcs0$
	14/02/2001	32	$2\farcs0$
	15/02/2001	38	$1\farcs8$
	16/02/2001	24	$1\farcs8$
	18/02/2001	1	$2\farcs5$
LAICA	23/01/2003	13	$3\farcs8$
	24/01/2003	19	$2\farcs5$
	25/01/2003	11	$2\farcs0$
	27/01/2003	22	$1\farcs5$
	28/01/2003	43	$1\farcs3$

The first time series was obtained using the 2-m Schmidt telescope at the Thüringer Landessternwarte Tautenburg (TLS, Germany), equipped with a 2048×2048 SiTe CCD camera. The wide-field camera provides a spatial resolution of $1\farcs2$/pixel, resulting in an unvignetted field of view of about 0.36 sqdeg. The observations at the TLS were carried out in two sessions in January and February 2001, with a gap of almost four weeks. Thus, although we cover more than a month in total, our sensitivity to long periods (1-4 weeks) will be limited. The observations were partly affected by cirrus and mediocre seeing conditions. In total, the run provided a time series of 125 images of the same field. The target field for the TLS run was centred at $\alpha = 8^h36^m53^s$, $\delta = +19°48'24''$ (J2000.0). This field contains nine members from the Hambly et al. catalogue (H85, 91, 102, 106, 115, 126, 140, 158, 181 in their nomenclature) and two from the Pinfield survey (P1 and P2 in their nomenclature), plus some more higher-mass members which are saturated in our images.

A second campaign was carried out using the wide-field imager LAICA at the 3.5-m telescope at Calar Alto Observatory from 23-28 Jan 2003 (in service mode). LAICA is a 2×2 mosaic of 4×4K CCDs, which we used to 'stare' at our target field in Praesepe. Thus, we did not observe a continuous field, but four 'patches' of $15' \times 15'$, separated by gaps of similar size, in total 0.25 sqdeg at a resolution of $0\farcs22$/pixel. The total length of the campaign was 10 nights (scheduled as 10 half nights), but most of the first half of the run was not useful due to excessively high seeing and cloud coverage. In the last six nights, however, we were able to obtain in total 108 images with mostly good quality. Thus, this time series will be highly sensitive to periods up to a few days. The LAICA run was focused on a target field at $\alpha = 8^h40^m56.5^s$, $\delta = +19°32'30''$ (J2000.0), not overlapping

[1] Based on observations collected at the Centro Astronomico Hispano Aleman (CAHA) at Calar Alto, operated jointly by the Max-Planck Institut für Astronomie and the Instituto de Astrofisica de Andalucia (CSIC), and at the Thüringer Landessternwarte Tautenburg (Germany)

with the TLS field. Since the LAICA images are considerably deeper than the TLS data, we aimed to cover some of the faintest member candidates in the cluster. The field thus contains six objects from the Pinfield survey (P14, 15, 16, 17, 19, 20) plus one additional unsaturated star from the Hambly list (H218).

2.2 From images to lightcurves

Image reduction, photometry, and relative calibration for both runs followed the routines established in the framework of our previous campaigns (Scholz & Eislöffel 2004a,b, 2005). In the following, we give a brief account of the basic principles of our method to derive lightcurves from time series images. For details, we refer to the more elaborated discussion in the afore mentioned papers, particularly Scholz & Eislöffel (2004a). In case of the LAICA campaign, all reduction and calibration steps were carried out separately on the four individual chips.

The image reduction started with bias subtraction and flatfield correction (based on high signal-to-noise domeflats). To remove the interference ('fringe') pattern produced by night sky line emission, which is typical for deep I-band exposures, we constructed a fringe mask (an image of the fringes, without objects) by averaging a number of dark sky exposures. This fringe mask was then properly scaled and subtracted from the individual time series images. Scaling is necessary because the amplitude of the fringes is a function of airmass and observing conditions. After this process, the residuals of the fringes in the final images do not exceed 1% of the sky background.

Using the Source Extractor, we created an object catalogue for one selected image in each time series ('master image'). Customised IRAF routines were used to a) determine pixel offsets between the master frame and all individual time series images, b) creating object catalogues for all time series images, c) carry out aperture photometry for all objects. For the TLS run, PSF fitting based on *daophot* was chosen as the optimum method for photometry. We selected a sample of PSF reference stars and used them to model the PSF in all time series images. Based on the values from the aperture photometry, new magnitudes were derived by adapting the model PSF to all objects in the field.

We refrained from using PSF fitting techniques for the LAICA run: Due to the strongly variable seeing conditions, it was not possible to find a set of PSF reference stars usable for a complete time series. Changing the reference PSF, however, may introduce systematic uncertainties. On the other hand, LAICA has an excellent pixel resolution, diminishing the benefits of PSF fitting photometry in moderately crowded fields. Therefore, we rely on the more robust aperture technique.

The instrumental magnitudes are still affected by the combined effects of varying airmass, varying atmospheric extinction, and variable zeropoint. This is corrected by subtracting a 'master lightcurve' from all time series, which is an average lightcurve calculated from a set of non-variable reference stars. The selection of these reference stars is the critical part in the relative calibration of the photometry. In a first step, we chose only objects with valid photometry and photometric error below 0.1 mag in all images. From this initial set (typically a few hundred objects), we excluded potentially variable objects by testing the rms in their lightcurve against the rms of all other preliminary reference stars. In several steps, the sample of reference stars is cleared from contaminating variable objects. For details of the process, we refer to Scholz & Eislöffel (2004a). After subtracting the resulting master lightcurve from all time series, we obtained lightcurves in relative magnitudes for all objects in our fields. This database is the fundament for the variability analysis described in Sect. 3.

We give two estimates for the accuracy of the relative calibration: a) The average rms of the final lightcurves of the reference stars (found to be non-variable) is 0.01 mag for the TLS and 0.02 mag for the LAICA run. b) The minimum rms measured from the lightcurves of bright stars is 0.009 mag in the TLS run and 0.01 mag for the LAICA run. Both methods provide an estimate of the intrinsic noise in the lightcurves. We conclude that for bright, but unsaturated objects we achieve a photometric accuracy of about 1% in both runs.

Table 2. Objects with significant periodic variability in Praesepe: Object ID (following Hambly et al. (1995b); Pinfield et al. (1997)), mass estimate (see Sect. 4.1), spectral type estimate (see Sect.4.1), period, period uncertainty, period amplitude

Object	M ($M_\odot$)	Sp.T.	P (h)	ΔP (h)	A (mag)
TLS:					
P2	0.12	M6.5	5.65	0.01	0.04
H91	0.29	M3	42.2	0.20	0.08
H115	0.40	M2	83.6	1.02	0.04
LAICA:					
P20	0.11	M7	12.2	0.20	0.07
H218	0.19	M4	16.2	0.51	0.04

3 PERIOD SEARCH

The main goal of the photometric monitoring was to detect periodic changes in the flux of our targets, which can be interpreted as indication of co-rotating spots – thus to measure rotation periods. The lightcurves of the Praesepe members in our fields were scrutinised with a rigorous period search procedure, which has been implemented and extensively tested in the framework of previous campaigns (Scholz & Eislöffel 2004a,b, 2005).

Period search in astronomic time series is non-trivial, mainly because of the characteristic gaps caused be daytime, weather changes, and unavailibility of the telescope. As a result, the distribution of datapoints is usually strongly clumped, hampering time series analysis. This is further complicated in the case of very low mass objects, where signal-to-noise (defined as ratio between amplitude of the periodic variation and noise level in the lightcurve) is typically less than five, so that the period is not always obvious from a by-eye examination. We try to mitigate these problems by a) maximising the number of datapoints in the lightcurve (to obtain as much information as possible about the light changes), and b) by probing for periodicities using a variety of independent and robust tests. In the following, we briefly outline the criteria which we require to be fulfilled to accept a period:

(i) The Scargle periodogram (Scargle 1982) shows

a peak with a preliminarily determined false alarm probability (FAP) below 1% (FAP calculated following Horne & Baliunas (1986)).

(ii) Nearby reference stars do not show the same peak in the periodogram.

(iii) The scatter in the lightcurve is significantly (based on a F-test) reduced after subtraction of the sine-wave approximated period.

(iv) The lightcurves of reference stars phased to the detected period do not show any sign of periodicity.

(v) The CLEAN algorithm (Roberts et al. 1987) confirms the periodogram peak, i.e. it is not an artefact from the window function.

(vi) The empirical FAP determined using a bootstrap approach (see below) is below 1%.

(vii) The phaseplot shows the period clearly (but see below).

Applying these criteria, we identified five objects with significant photometric period in the lightcurve (see Table 2). The phaseplots for these five objects are shown in Fig. 1. Please see below for individual notes on the lightcurves. Final values for the FAP have been determined using the bootstrap approach explained in detail in Scholz & Eislöffel (2004a). The basic idea is to produce 10000 randomised lightcurves per object by retaining the observing times and shuffling the data-values only. The resulting lightcurves will have the same sampling and noise level as the original time series, but certainly no periodicity. For all 10000 random lightcurves we calculated the Scargle periodogram and determined the amplitude of the highest peak. The fraction of lightcurves, for which this number exceeds the peak amplitude for the *measured* periodicity of the given object is a robust and reliable estimate for the FAP for this period. For all five detected periods, the peak in the periodogram is clearly higher than any peak from the 10000 randomised lightcurves; thus the FAP is below 0.01%.

We tested the range of periods for which we are sensitive by adding sinewaves with typical amplitudes of 0.05 mag and varying period to the lightcurves of non-variable reference stars. By applying the period search procedure used for our target stars to these 'artificial' periodic objects, we find that our sampling allows us to reliably detect periods between $\sim$ 1 h and $\sim$ 4 days (in both runs). This is in line with the expectations: Both monitoring campaigns provided dense sampling over at least three consecutive nights, with only spotty coverage for longer timescales. Hence, it is not surprising that all our five detected periods are in the range between 1-4 d. However, it has to be emphasised that the period search is not sensitive for periods around multiples of 1 day, due to the daytime gaps, thus the period sample is probably not complete. On the other hand, both time series have some potential to detect periods longer than 4 days (up to periods of a month for the TLS run). Still, given the fact that our sensitivity for these long periods is limited, we do not put too much emphasis on the fact that we did not find any such period.

Our period search still includes one subjective criterium: the by-eye examination of the phased lightcurves. We require that the period is visible in this plot, i.e. that it shows a clear maximum and minimum. However, this criterium has to be used with caution. As we have

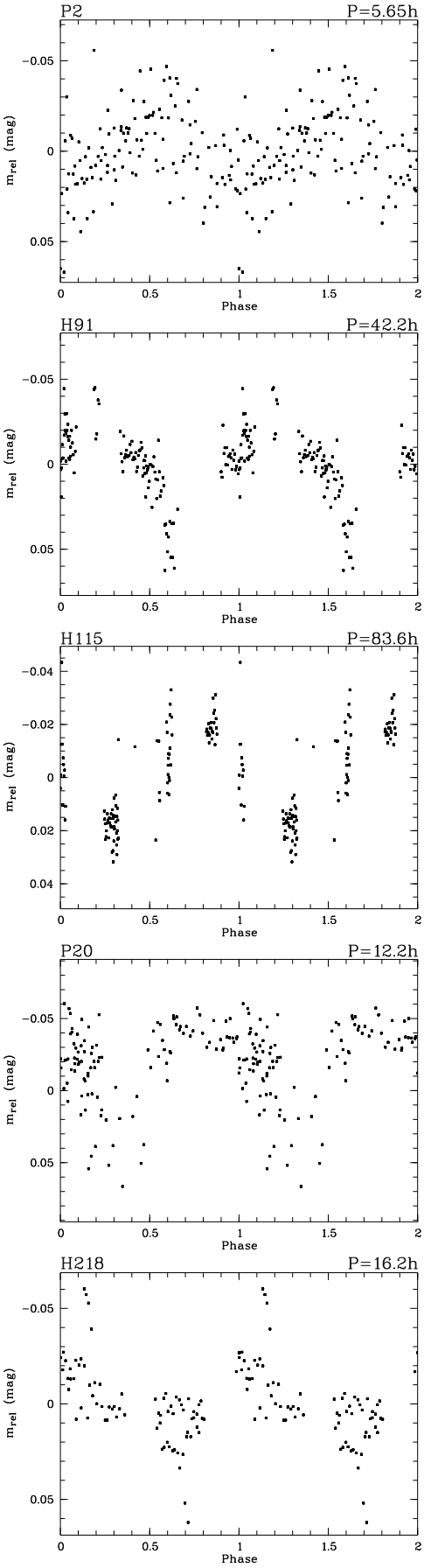

Figure 1. Phase plots for the five objects with significant periodic variations. P2, H91, H115 have been observed in the TLS run, P20 and H218 in the LAICA run .

shown in Scholz & Eislöffel (2005), periodogram techniques are able to pick up periods even at signal-to-noise levels too low to produce a visually obvious periodicity in the lightcurve. Thus, a not entirely convincing phaseplot (see Fig. 1) does not necessarily indicate a false detection. This has to be taken into account when discussing individual objects. Please note that the objects P2, H115, and P20 have been confirmed as cluster members by near-infrared photometry (Hodgkin et al. 1999). Based on their position in the colour-magnitude diagram, P2 and H115 have been classified as possible binaries.

Notes on individual objects:

P2: The object is one of the faintest, lowest mass members of Praesepe discovered so far. We estimate roughly $0.1\,M_{\odot}$; if the object really is a binary, this corresponds to the total system mass. Additionally, the amplitude of the periodicity if fairly low, resulting in low signal-to-noise ratio. This is a typical case where the effects of the low signal-to-noise are offset by a large number of datapoints (in this case 123). Scargle and CLEAN periodogram show a convincing peak, which translates into a highly significant period of 5.65 h.

H91: Although the phaseplot for the period of 42.2 h exhibits some gaps, the datapoints do show a clear flux modulation, i.e. maximum and minimum are clearly visible.

H115: Due to the relatively long period of 83.6 h, the coverage is not continuous. The two strong clumps at phases of 0.3 and 0.85 represent the datapoints from Feb 14 and 16, respectively, which are clearly offset by roughly 0.04 mag, and thus give direct evidence for a photometric variation on timescales of days.

P20: The phaseplot shows a clear periodicity, but the lightcurve appears 'box'-shaped. This raises the question whether we are dealing with an eclipsing binary rather than a rotational modulation. However, when examining the lightcurve, there are clear smooth and gradual trends in some nights rather than rapid brightness changes, which is difficult to explain in an eclipse scenario. Moreover, the fact that the suspected eclipse covers almost half of the phase space would require a roughly equal-radius binary system, which is unlikely given the very small eclipse depth. Moreover, the period would imply an orbital separation of fractions of 1 AU, and such systems seem to be rare (Fischer & Marcy 1992). Therefore, we attribute the 'boxy' shape of the lightcurve to an unusual spot configuration. Still, the possibility of an eclipsing system cannot completely be disregarded.

H218: The largest peak in the Scargle periodogram corresponds to a period of 33.6 h, but disappears after applying the CLEAN routine and is thus probably an artefact. CLEAN, however, identifies a peak at the doubled frequency (corresponding to a period of 16.2 h) as real. Since the same peak is also highly significant in the Scargle periodogram, we adopt a period of 16.2 h for this object. The period remains significant when we exclude the five outlying datapoints at phases of 0.15 and 0.7.

4 INTERPRETATION

The best explanation for the observed periodic variability is the presence of spots on the surface of the stars, co-rotating with the objects and thus modulating the flux. With an idealised spot distribution (one spot, regularly shaped), we would expect sine-shaped periodicities, particularly at low signal-to-noise ratio. In contrast, other sources of periodic variations (eclipsing binaries, planetary transits) produce regular dips in the lightcurves. Four out of five periods clearly resemble a sinecurve. The sole exception, P20, could be an eclipsing binary, but we argue that its box-shaped lightcurve is more likely caused by a particular distribution of surface features.

The underlying reason of the surface features is most likely magnetic activity: Our targets have effective temperatures larger than 3000 K (spectral types around mid M), rendering the possibility of condensated dust clouds, as often discussed for the much cooler L dwarfs, improbable. M dwarfs, on the other hand, are known to harbour substantial magnetic fields, as evidenced by X-ray and Hα activity. Specifically, for three of our periodic objects (H91, H115, H218) chromospheric activity evidenced by Hα emission with equivalent widths between 3 and 23 Å has been reported by Barrado y Navascués et al. (1998) and Kafka & Honeycutt (2006). It seems reasonable to assume that the remaining two objects (without Hα observation so far) share similar chromospheric properties.

Thus, for the following discussion, we assume that the most likely origin for the observed periodic variations is a rotational modulation due to magnetically induced surface spots. Hence, the periods correspond to the rotation periods of our targets. These are the first rotation periods measured for objects in this mass range in a cluster significantly older than the ZAMS stage (which is reached at roughly 0.2-0.3 Gyr for very low mass stars, see Irwin et al. (2007)). In the following subsections, we will use this small period sample in combination with literature data to probe rotation vs. mass and rotation vs. age for very low mass objects on the main-sequence.

To assure ourselves that the five datapoints give a realistic first glance of the VLM period distribution in Praesepe, we carried out two plausibility checks. First, we compare with $v \sin i$ values for the Hyades, compiled by Terndrup et al. (2000). The Hyades are roughly coeval with Praesepe, and since the $v \sin i$ sample size in the very low mass range is about 20, these values can provide a useful consistency check. In the mass range 0.2-0.4 $M_{\odot}$, the lower limit in rotational velocities is defined by the detection limit of $5\,\mathrm{km s^{-1}}$, which translates to an upper limit in $P \sin i$ of 30-90 h, depending on mass (with radii from Chabrier & Baraffe (1997)). The upper limit in $v \sin i$ is around $15\,\mathrm{km s^{-1}}$, corresponding to a lower limit for $P \sin i$ between 10 and 30 h. Considering that $\sin i$ has a fairly tight distribution around 0.7-0.8 for random orientations of rotational axes, these numbers are completely consistent with our period limits.

A second check can be made based on the period ranges for clusters somewhat younger than Praesepe. In the Pleiades, NGC2516, and M34, all clusters with ages between 100 and 200 Myr, a substantial sample of VLM periods has been established, in total $\sim$ 300, the dominant majority in NGC2516 (Irwin et al. 2006, 2007; Scholz & Eislöffel 2004b). These periods range from 3 h to about 3 days. Given the fact that there is no known mechanism to accelerate rotation on the main-sequence, instead, we expect rotational

braking and thus longer periods in older clusters, this again seems consistent with the period range in Praesepe. A more detailed analysis of the rotational evolution based on a comparison of Praesepe with younger clusters will be given in Sect. 4.2. Here we conclude that the small sample in Praesepe is likely to represent a typical range of VLM rotation periods in this cluster.

4.1 Rotation vs. mass

It is well-established that rotation is a function of object mass (see Herbst et al. 2007, for a review). Specifically, there is accumulating evidence that in the very low mass regime the average period drops steadily with decreasing mass. This positive period-mass correlation at masses $< 0.3 - 0.4\,M_{\odot}$ has been found in the ONC (Herbst et al. 2001), ϵ Ori (Scholz & Eislöffel 2005), and the Pleiades (Scholz & Eislöffel 2004b), clusters with ages between 1 and 125 Myr. Similarly, in the clusters NGC2516 and M34 (Irwin et al. 2006, 2007), which roughly mark the ZAMS for very low mass objects at ages of 150 and 200 Myr, there seems to be a general decline of the upper envelope of the periods with decreasing mass (Irwin et al. 2007, see their Fig. 17). It has been pointed out that this trend is consistent with constant angular momentum for all object masses (e.g. Herbst et al. 2001), and thus might just reflect the drop in stellar radius. Since it is already established at very young ages, it may be related to the initial distribution of angular momentum.

Here we probe if our small period sample in Praesepe – older than all other clusters with rotation periods in this mass range – allows us to see a similar trend. We derived masses for the five objects in Table 2 by comparing the available photometry in the I-band from the literature with evolutionary tracks from Baraffe et al. (1998) for an age of 0.75 Gyr. According to these estimates, all five objects are in the very low mass regime with masses $\leqslant 0.4\,M_{\odot}$. Due to age uncertainties, photometric band inconsistencies, and model shortcomings, the uncertainties in the derived masses are considerable (probably on the order of 50%). However, most of this uncertainty is systematic, thus we expect that in a relative sense our masses are realistic. We caution against comparing these values with masses derived using a different approach. Using the same model isochrone, we determined effective temperatures for our five targets. Comparing with the $T_{\rm eff}$ scale from Luhman et al. (2003) gives an estimate for the spectral types (see Table 2). The uncertainties in these 'photometric' spectral types are probably $\pm 1 - 2$ subclasses.

In Fig. 2, upper panel, we plot periods vs. masses for the five objects in Table 2. It is immediately obvious that the periods appear to increase with mass in a roughly linear way. A linear least-square fit (shown as dotted line) gives: $P = (240 \pm 40)\,(M/M_{\odot}) - (21 \pm 10)\,h$. The correlation is significant with a false alarm probability of 1.0%. The slope in the relationship is clearly steeper than in the Pleiades ($105 \pm 61\,(M/M_{\odot})$, Scholz & Eislöffel (2004b)), maybe indicating that rotational braking on the main-sequence is a function of object mass. Based on only five datapoints, however, this finding is of somewhat limited value. Clearly, more

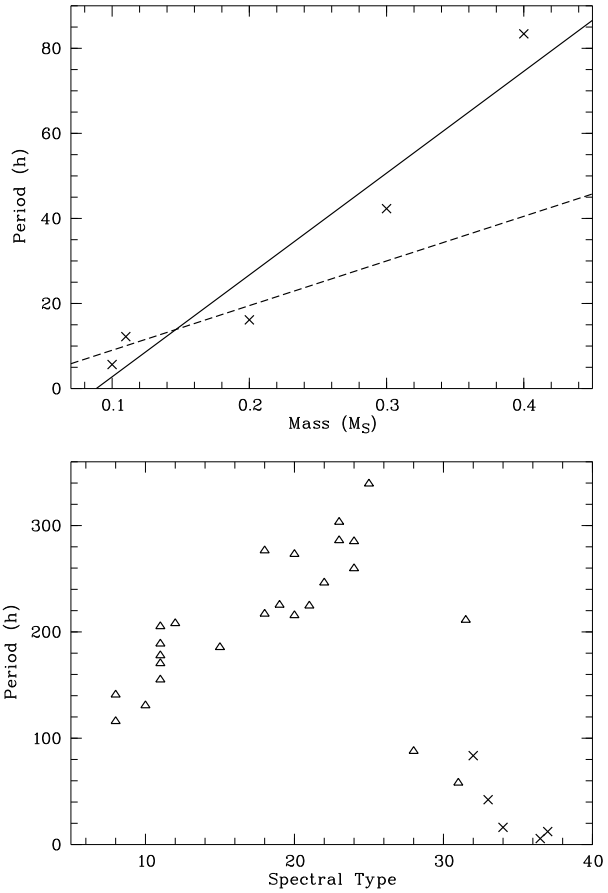

Figure 2. Upper panel: Rotation period vs. mass for VLM objects in Praesepe. The solid line is a linear fit; the dashed line shows the P(M) fit for our VLM period sample in the Pleiades (Scholz & Eislöffel 2004b). **Lower panel:** Rotation period vs. spectral type (as indicator for mass): Crosses are the five VLM periods in Praesepe from this work, triangles are periods in the coeval Hyades from Radick et al. (1987) and Prosser et al. (1995). Spectral type is parameterised as follows: G0 – 10, K0 – 20, M0 – 30.

datapoints are needed to solidify the main-sequence P-M correlation in the VLM regime.[2]

It is more instructive to look on the VLM periods in comparison with rotation measurements obtained for more massive stars. To our knowledge, such data is not available for Praesepe, but for the Hyades, with 600 Myr a roughly coeval cluster (Mermilliod 1981; Perryman et al. 1998). For this comparison, we prefer to use spectral types instead of masses, in order not to be biased by model inconsistencies in the mass estimates, which are difficult to avoid when covering a mass range of more than one order of magnitude. Since we use only coeval objects, the spectral type is a valid indicator for stellar mass. We collected a sample of 25 periods for Hyades members from the photomet-

[2] We note that for the three objects with published Hα equivalent widths the rotation periods seem to decline with increasing activity, so it may be that the observed period-mass trend is in fact a reflection of activity levels increasing with later spectral types.

ric monitoring campaigns published by Radick et al. (1987) and Prosser et al. (1995). Spectral types for these objects have originally been published by van Bueren (1952) and van Altena (1969). Combined with our sample, the spectral range from late F to late M is covered, roughly corresponding to a mass range from 0.1 to 2 $M_\odot$.

The period/spectral type relation is shown in Fig. 2, lower panel. It clearly demonstrates that for F-K stars the periods increase towards later spectral types. According to Radick et al. (1987), these periods can be explained in terms of the correlation between magnetic activity and the inverse Rossby number *Ro*, the ratio between rotation period and convective turnover timescale τ_C (e.g. Noyes et al. 1984). This relation basically implies that the magnetic field amplification mainly depends on convection properties and rotation – supporting the idea of an $\alpha\omega$ dynamo operating in F-K stars. We note that the Hyades periods for F-K stars represent what Barnes (2003) called the I-sequence of rotational evolution, i.e. objects with interface dynamo.

As it is apparent from Fig. 2, this sequence breaks down roughly at spectral types K8-M2, corresponding to a mass of about 0.4-0.6 $M_\odot$ (or a $B-V$ colour > 1.5). Without clear transition regime, the periods drop by almost one order of magnitude between K8 and M2. Even if the period distribution at very low masses is not complete (but see above), the simple fact that the fast rotators do exist among M dwarfs and not in the G-K spectral range indicates a fundamental change in stellar rotation at the given mass limit.

The underlying physical reason for this breakdown is not clear. Obviously, it indicates a dramatic change in the rotational braking at a certain mass, which may be related to a change in wind properties, surface magnetic field, or dynamo action. It should be noted that the break in rotation period in Praesepe occurs roughly at the same spectral type as the onset of chromospheric activity measured as Hα emission: As recently reported by Kafka & Honeycutt (2006), Praesepe objects earlier than M1 are rarely chromospherically active, in contrast to later type objects. Since enhanced activity would normally be associated with the potential of efficient angular momentum loss, this poses the question why the fast rotating M-dwarfs in Praesepe are the most active objects.

In the rotational evolution scheme by Barnes (2003), the fast rotating M-dwarfs in Praesepe would represent the C-sequence (quote: 'possess only a convective field', 'no large scale dynamos'). In this view, the mass limit at which I-sequence and C-sequence bifurcate should be a function of age and shift to later spectral types as objects get older. There is indeed some evidence for this: In $v \sin i$ data for field M dwarfs, most of them certainly older than Praesepe, the fraction of fast rotators increases from zero at M3 to 100% at M6 (Delfosse et al. 1998), clearly at lower masses than the transition seen in Praesepe/Hyades. Still, this does not explain *why* the magnetic field and the dynamo, as suggested by Barnes (2003), should change abruptly at a given mass.

Is there a link between the rotational properties and the interior structure of the stars in the VLM range? Objects with 0.5 $M_\odot$ are still thought to harbour a substantial radiative core (Chabrier & Baraffe 1997). Going to lower masses, however, the bottom of the convective envelope drops quickly until the objects are fully-convective. There is strong reason to believe that dynamo action changes in a fundamental way with the disappearance of the radiative core. The $\alpha\omega$ dynamo ('interface dynamo') thought to operate in solar-type stars requires a shear layer at the bottom of the convection zone, which is not supposed to exist in fully convective objects. Thus, it can be expected that the F-K type activity vs. *Ro* relation breaks down as soon as the radiative core disappears. At the same time, the objects may lose the ability of efficient rotational braking, possibly due to a change from large-scale to small-scale fields, resulting in fast rotators.

However, structural models of low-mass stars essentially agree on the fact that this transition is supposed to occur at masses between 0.3 and 0.4 $M_\odot$ for $M/H = -2 \ldots 0$ (e.g. Chabrier & Baraffe 1997; Montalbán et al. 2000) or even below (Mullan & MacDonald 2001), i.e. at lower masses than the observed drop in rotation periods apparent in Fig. 2. This limit depends on metallicity in a complex way and is expected to increase somewhat for $M/H > 0$ (Chabrier & Baraffe 1997). Since both Hyades and Praesepe have higher than solar metallicities (M/H of 0.17 and 0.14 respectively), this might account for some of the the difference in object mass between observed and expected transition to fast rotators. If the break in the mass-period relation is entirely to explain with the change to fully convective objects, however, remains questionable.

The appearance of Fig. 2 and its possible potential to probe magnetic and structural properties is intriguing enough to justify future research to explain its origin. The following approaches appear to be particularly useful: a) modeling the transition to fully convective objects for a range of metallicities, b) complementary observations in the K8-M2 spectral range to check for changes in magnetic properties (e.g., Doppler imaging, magnetic field measurements, multi-wavelength monitoring), c) rotational studies for stars with masses between 0.6 and 0.3 $M_\odot$, which are so far only represented by 4 datapoints.

4.2 Rotation vs. age

The rotational evolution of stars is believed to be controled by mainly three mechanisms:
a) disk braking, i.e. angular momentum losses due to coupling between star and circumstellar disk, for example as so-called 'disk-locking' (see the review by Herbst et al. 2007),
b) pre-main sequence contraction resulting in a spin-up,
c) magnetic winds driven by dynamo actions, carrying away mass and angular momentum.

In Fig. 3, we compare our rotation periods for Praesepe with period data for VLM objects in younger clusters: eleven rotation periods for stars in the Pleiades (age 125 Myr), (Scholz & Eislöffel 2004b; Terndrup et al. 1999), about 250 periods for objects NGC2516 (age 150 Myr) shown as median, 10%, and 90% percentiles (Irwin et al. 2007), nine periods in M34 (age 200 Myr, Irwin et al. (2006). Together with the five Praesepe periods, this is to our knowledge the total available period data for main-sequence VLM stars. In all four clusters, the sampling of the photometric monitoring was sensitive to periods ranging from $\leqslant$ 30 min to at least four days. In the Pleiades and M34, the detection range extends to 12 and $\sim$ 10 days, respectively. To illustrate the differences in the mass ranges, objects with $0.2 < M < 0.4\,M_\odot$ are shown as plus signs and lower mass

objects as crosses. Note that the majority ($\sim$ 90%) of the periods in NGC2516 has been obtained for stars in the upper mass bin. For Praesepe, we use here an age of 650 Myr, as given by Mermilliod (1981); shifting the datapoints within 600-900 Myr (the likely age range for the cluster) does not affect the following results.

We calculated simple rotational evolutionary tracks taking into account spin-up due to contraction and angular momentum losses by stellar winds. Since typical disk lifetimes are < 10 Myr, the influence of disk braking is irrelevant here. The spin-up was estimated using radii from the models of Chabrier & Baraffe (1997). Since even the lowest mass objects have reached their final radii to within 10% after 200 Myr, the effect of contraction of the rotation period is only visible between 100 and 200 Myr. After that, the rotational evolution is almost entirely determined by braking due to stellar winds – that's why main-sequence clusters are the ideal environment to test wind braking. For solar-type stars, wind braking results in the so-called Skumanich law (Skumanich 1972): $P \propto \sqrt{t}$. In Scholz & Eislöffel (2004b) we demonstrated that this braking law is not applicable in the pre-main sequence evolution of VLM objects, because it predicts periods > 4 days at ~ 100 Myr, while the upper VLM period limit at this age, reliably determined from the available period and $v \sin i$ data, is only ~ 2 days. Thus, a more moderate braking law has to be used, as it is expected for objects with saturated dynamo (Terndrup et al. 2000; Barnes 2003) or for objects with a strong concentration of magnetic flux near the pole (Solanki et al. 1997). We use here an exponential form for the braking law $P \propto \exp(t)$, as it is expected for a saturated dynamo. Given the lack of understanding for the underlying physics for this type of rotational braking, this should be treated as an ad-hoc solution to provide moderate braking, rather than an accurate physical model.

Taken together, the rotational evolution can be expressed as: (R_i: initial radius, R_f: final radius, P_i: initial period)

$$P_f = \alpha \times (R_i/R_f)^2 \times P_i \quad (1)$$

with $\alpha = 1$ for zero wind braking and $\alpha = \exp(t/\tau)$ for exponential braking, where τ is the braking (or spin-down) timescale. In Fig. 3 we plot both cases, no braking with dotted lines, exponential braking with dashed lines. The rotational evolution is shown for $0.4\,M_\odot$, starting at $P_i = 40$ h (upper limit in the Pleiades) and $0.1\,M_\odot$, starting $P_i = 3$ h (lower limit in the Pleiades). The different values for P_i were chosen to reflect the P-M relationship discussed in Sect. 4.1. As can be seen from the tracks, changing the mass does not significantly affect model tracks.

In the discussion of this plot, it is important not to be misguided by the small number of periods. In particular, it is essential to keep in mind that the Praesepe period range is probably incomplete (in contrast to the younger clusters). Thus, rather than reproducing upper and lower period limits, the rotational evolutionary tracks should simply be able to explain the *existence* of the periods measured in Praesepe.

As can be seen in Fig. 3, tracks without any braking on the main sequence (dotted lines) have problems reproducing the longest periods measured so far in NGC2516, M34, and Praesepe. Thus, some rotational braking on the main-sequence is likely occuring among VLM objects, in agreement with our findings in Scholz & Eislöffel (2004b). From the tracks for exponential braking, we can rule out that the braking timescale τ is shorter than 200 Myr: Such low values for τ would imply that an object with 3 h rotation period at 100 Myr (lower limit in the Pleiades) has a period longer than 100 h at the age of Praesepe – thus not allowing for any of our five measured periods. The plausible range for the braking timescales is between 400 Myr and 800 Gyr (in Fig. 3 we show the tracks for $\tau = 600$ Myr). [3]

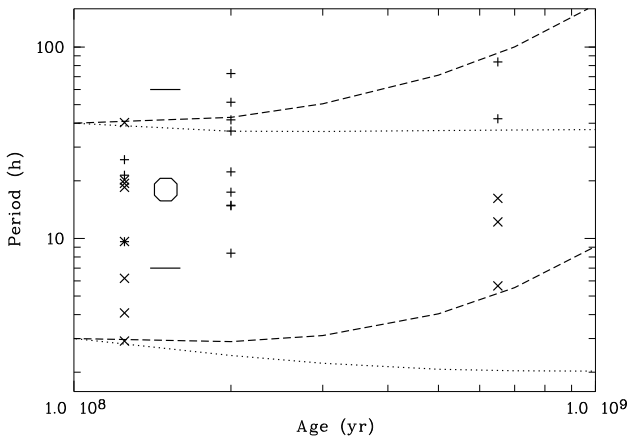

Figure 3. Rotation periods for $0.1 - 0.4\,M_\odot$ mass objects in Pleiades, NGC2516, M34 (Scholz & Eislöffel 2004b; Irwin et al. 2006, 2007), and Praesepe (this paper). We chose different symbols for two mass bins: $0.2 - 0.4\,M_\odot$ – plus (+), $0.1 - 0.2\,M_\odot$ – cross (x). For NGC2516, we plot the median as octagon and the 10%- and 90%-percentiles as horizontal lines. Note that the upper period limits in Pleiades, M34, and NGC2516 are reliably determined, while the period range in Praesepe may be incomplete. The dotted lines show the period evolution as expected for zero wind braking. Dashed lines include exponential wind braking with $\tau = 600$ Myr.

These results are mostly consistent with earlier findings for the spin-down timescale in the VLM regime. In Scholz & Eislöffel (2004b) we conclude that the rotational braking in the VLM regime occurs on timescales of a 'few hundred Myrs'. Consistently, Terndrup et al. (2000) find a value of $\tau = 246 \pm 55$ Myr from a comparison of $v \sin i$ in Pleiades and Hyades. Several studies point to spin-down timescales in the range of or larger than 1 Gyr (Delfosse et al. 1998; Sills et al. 2000; Barnes 2003). All these estimates are in order-of-magnitude agreement with our new constraint. Taken together, the available rotational data for VLM objects favours the occurence of weak rotational braking on the main-sequence, with exponential spin-

[3] Based on the currently available data, it appears that the period ranges in M34 and Praesepe are indistinguishable. If this is indeed the case, most of the rotational braking in the VLM range would occur at ages < 200 Myr. The spindown would be more rapid until about the age of M34 and would slow down considerably after that. While such a time-dependent spindown is certainly an interesting scenario, we do not put too much trust in this interpretation, because low number statistics and period incompleteness in Praesepe might easily be responsible for the effect. In addition, the mass ranges for the objects with periods differ slightly from cluster to cluster, which in combination with the strong period-mass relation (see Sect. 4.1) can lead to biases.

down timescales larger than 200 Myr, maybe as long as a few Gyrs.

According to Barnes (2003), the spin-down timescales for fast rotating G-stars in young open clusters are $\sim$ 30 Myr. Thus, among VLM objects, the spin-down happens at a much slower rate than for solar-mass stars: the braking timescales are 10-100 times longer. This results in fast rotating main-sequence objects, as already evidenced by the rotation vs. mass plot in Sect. 4.1. Both findings, the steep drop in rotation periods and the similarly steep increase in the spin-down timescales, are complementary observational manifestation of a fundamental change in the angular momentum regulation in the VLM regime.

5 SUMMARY AND OUTLOOK

Rotation periods have been measured from photometric monitoring for five stars in the open cluster Praesepe (age $\sim$750 Myr), all with masses $< 0.5\,M_{\odot}$. Our work demonstrates that it is possible to obtain reliable periods for faint objects at the bottom of the main-sequence using wide-field imagers at medium-sized telescopes, as long as enough observing time is available to provide a large number of datapoints and thus a high level of redundancy. We show that main-sequence open clusters like Praesepe are ideal environments to probe the long-term angular momentum evolution and the underlying regulation mechanisms.

The five periods range from 5 h to almost 3.5 days and have been confirmed by various independent period search procedures as well as plausibility checks. We attribute these photometric variations to cool, magnetically induced spots, co-rotating with the objects – thus the periods likely correspond to the rotation periods. Comparing the small sample of periods in Praesepe with $v \sin i$ data for the coeval Hyades and with periods measured in younger clusters, we conclude that they give a reasonable first glance on the very low mass (VLM) period distribution in Praesepe. Particularly, it is unlikely that Praesepe harbours a large, undetected population of VLM objects with periods significantly longer than 4 days. Still, the big caveat in the discussion of the periods is the small number of datapoints. As long as we do not have a more substantial dataset, we refrain from carrying out a vigorous statistical analysis and rely instead on more qualitative assessments.

We find a trend of decreasing period with decreasing mass in the VLM regime, confirming previous claims in younger clusters. This trend is roughly linear in our small sample with $P \approx 240\,(M/M_{\odot})\,h$. To probe the period-mass relation over a broad range of stellar masses, we combine our dataset with periods in the coeval Hyades from the literature. We find a dramatic change in the periods at spectral type K8-M2, corresponding to masses of 0.4-0.6 $M_{\odot}$: Without clear transition regime, the periods drop from $\sim$ 10 days in mid K-stars to $<$ 4 days in early M-stars. Even considering that the VLM period sample may be incomplete, the mere existence of the fast rotating M-dwarfs in Praesepe indicates a significant change in the rotational regulation. We note that this change coincides with the onset of chromospheric activity occuring at spectral type M1 in Praesepe (Kafka & Honeycutt 2006).

Comparing the periods in Praesepe with rotational data in younger clusters (ages of 100-200 Myr), we find that some angular momentum loss is likely to occur in the VLM range. The exponential timescale of spin-down due to stellar winds is clearly longer than 200 Myr, most likely between 400 and 800 Myr, and thus 10-100 times longer than in solar-mass stars. Hence, rotational braking on the main-sequence is clearly less efficient in the VLM regime, resulting in fast rotators.

Thus, the periods in Praesepe provide evidence for two observational manifestations of a fundamental change in the rotational regulation: a clear drop of the rotation periods at 0.4-0.6 $M_{\odot}$ and very long spin-down timescales in the VLM regime. This is in line with previous findings: Sills et al. (2000) made an attempt to model the rotational evolution of VLM objects and conclude that it is impossible to 'simultaneously reproduce the observed stellar spin-down in the $0.6 - 1.1\,M_{\odot}$ range and for stars between 0.1 and $0.6\,M_{\odot}$', implying that the solar-type rotational models are not applicable at very low masses. In the evolutionary scheme proposed by Barnes (2003), the break between 'I- and C-sequence' (which is identical to the break in the period-mass relation reported in this work) can be seen as another way to describe a transition between two different rotational regulation regimes. In summary, the solar-type rotational evolution picture of a transition dynamo driving a magnetic wind, which leads to Skumanich-type angular momentum losses, does not appear to be applicable in the VLM regime.

The underlying physical reason for this fundamental breakdown of the solar-type rotational braking is not clear. We argue that it might be possible to explain it with the disappearance of the radiative core and the resulting inability to operate a solar-type interface dynamo. However, this transition is thought to occur at masses 0.3-0.4 $M_{\odot}$ in solar-metallicity stars, i.e at somewhat lower masses than the drop in rotation periods. The metallicity difference between the Sun and young clusters like Praesepe might explain parts of this discrepancy. Fundamental changes in the magnetic field structure, the wind properties, or dynamo action (possibly independent of interior structure) have to be considered as alternative ways to understand the observational findings.

The obvious signature of a fundamental change seen in the rotation periods holds great potential to use rotation as a probe for magnetic properties and/or interior structure. Follow-up studies aimed a) to enlarge the rotational database for VLM objects on the main-sequence and b) to provide complementary activity-related data in this mass regime are thus highly desirable to clarify the open questions.

ACKNOWLEDGMENTS

We thank the referee for a constructive review. AS would like to thank Andrew Collier Cameron, Volkmar Holzwarth, and Jerome Bouvier for instructive discussions regarding topics related to this paper. This study benefited from unbureaucratic scheduling of observing time by Ulli Thiele, Astronomy Department Head at Calar Alto Observatory, and Artie Hatzes, Director at the TLS Tautenburg. We gratefully acknowledge the efforts of the observers at the TLS Tautenburg (Christian Högner, Uwe Laux, Frank Ludwig) and Calar Alto Observatory (Ana Guijarro, Nicolas

Cardiel, Manuel Alises, Jesus Aceituno) to provide high-quality data even under often not perfect conditions. This work was partially supported by *Deutsche Forschungsgemeinschaft* (DFG) grant Ei 409/11-1 and 11-2.

REFERENCES

Adams J. D., Stauffer J. R., Skrutskie M. F., Monet D. G., Portegies Zwart S. F., Janes K. A., Beichman C. A., 2002, AJ, 124, 1570
Baraffe I., Chabrier G., Allard F., Hauschildt P. H., 1998, A&A, 337, 403
Barnes S. A., 2001, ApJ, 561, 1095
—, 2003, ApJ, 586, 464
Barrado y Navascués D., Stauffer J. R., Randich S., 1998, ApJ, 506, 347
Chabrier G., Baraffe I., 1997, A&A, 327, 1039
Delfosse X., Forveille T., Perrier C., Mayor M., 1998, A&A, 331, 581
Fischer D. A., Marcy G. W., 1992, ApJ, 396, 178
Hambly N. C., Steele I. A., Hawkins M. R. S., Jameson R. F., 1995a, MNRAS, 273, 505
—, 1995b, A&AS, 109, 29
Herbst W., Bailer-Jones C. A. L., Mundt R., 2001, ApJ, 554, L197
Herbst W., Eislöffel J., Mundt R., Scholz A., 2007, Protostars and Planets V, 297
Hodgkin S. T., Pinfield D. J., Jameson R. F., Steele I. A., Cossburn M. R., Hambly N. C., 1999, MNRAS, 310, 87
Horne J. H., Baliunas S. L., 1986, ApJ, 302, 757
Irwin J., Aigrain S., Hodgkin S., Irwin M., Bouvier J., Clarke C., Hebb L., Moraux E., 2006, MNRAS, 370, 954
Irwin J., Hodgkin S., Aigrain S., Hebb L., Bouvier J., Clarke C., Moraux E., Bramich D. M., 2007, MNRAS, 276
Kafka S., Honeycutt R. K., 2006, AJ, 132, 1517
Luhman K. L., Stauffer J. R., Muench A. A., Rieke G. H., Lada E. A., Bouvier J., Lada C. J., 2003, ApJ, 593, 1093
Magazzu A., Rebolo R., Zapatero Osorio M. R., Martin E. L., Hodgkin S. T., 1998, ApJ, 497, L47+
Mermilliod J. C., 1981, A&A, 97, 235
Montalbán J., D'Antona F., Mazzitelli I., 2000, A&A, 360, 935
Mullan D. J., MacDonald J., 2001, ApJ, 559, 353
Noyes R. W., Hartmann L. W., Baliunas S. L., Duncan D. K., Vaughan A. H., 1984, ApJ, 279, 763
Perryman M. A. C., Brown A. G. A., Lebreton Y., Gomez A., Turon C., de Strobel G. C., Mermilliod J. C., Robichon N., Kovalevsky J., Crifo F., 1998, A&A, 331, 81
Pinfield D. J., Hodgkin S. T., Jameson R. F., Cossburn M. R., von Hippel T., 1997, MNRAS, 287, 180
Prosser C. F., Shetrone M. D., Dasgupta A., Backman D. E., Laaksonen B. D., Baker S. W., Marschall L. A., Whitney B. A., Kuijken K., Stauffer J. R., 1995, PASP, 107, 211
Radick R. R., Thompson D. T., Lockwood G. W., Duncan D. K., Baggett W. E., 1987, ApJ, 321, 459
Roberts D. H., Lehar J., Dreher J. W., 1987, AJ, 93, 968
Robichon N., Arenou F., Mermilliod J.-C., Turon C., 1999, A&A, 345, 471
Scargle J. D., 1982, ApJ, 263, 835
Scholz A., Eislöffel J., 2004a, A&A, 419, 249
—, 2004b, A&A, 421, 259
—, 2005, A&A, 429, 1007
Schrijver C. J., Zwaan C., 2000, Solar and Stellar Magnetic Activity. Solar and stellar magnetic activity / Carolus J. Schrijver, Cornelius Zwaan. New York : Cambridge University Press, 2000. (Cambridge astrophysics series ; 34)
Sills A., Pinsonneault M. H., Terndrup D. M., 2000, ApJ, 534, 335
Skumanich A., 1972, ApJ, 171, 565
Solanki S. K., Motamen S., Keppens R., 1997, A&A, 324, 943
Stauffer J. R., Hartmann L. W., Prosser C. F., Randich S., Balachandran S., Patten B. M., Simon T., Giampapa M., 1997, ApJ, 479, 776
Terndrup D. M., Krishnamurthi A., Pinsonneault M. H., Stauffer J. R., 1999, AJ, 118, 1814
Terndrup D. M., Stauffer J. R., Pinsonneault M. H., Sills A., Yuan Y., Jones B. F., Fischer D., Krishnamurthi A., 2000, AJ, 119, 1303
van Altena W. F., 1969, AJ, 74, 2
van Bueren H. G., 1952, Bulletin of the Astronomical Institutes of the Netherlands, 11, 385